AIAA

AIAA 93-2081
Propellant Reorientation Effects on the Attitude of the Main Cryotechnic Stage of ArianeV

Y.Letourneur
Aerospatiale
Les Mureaux, France

J.Sicilian
Flow Science Inc.
Los Alamos, New Mexico

AIAA/SAE/ASME/ASEE
29th Joint Propulsion
Conference and Exhibit
June 28-30, 1993 / Monterey, CA

PROPELLANT REORIENTATION EFFECTS ON THE ATTITUDE OF THE MAIN CRYOTECHNIC STAGE OF ARIANEV

Y.Letourneur, Aerospatiale, Les Mureaux (France)
J.Sicilian, Flow Science Inc., Los Alamos (New Mexico)

Abstract

The objective of this study, performed in the frame of the ArianeV program, is to determine the attitude of the Main Cryotechnic Stage (EPC) of the launcher when it is spun after the staging with the Upper stage. The liquids contained in the LOX and LH2 tanks are likely to affect this spin-up. Therefore, an analysis of the propellant reorientation was undertaken using the code FLOW-3D (ref.1), then a simplified model, which includes a coupled (fluid/dry vehicle) dynamics computation , was used to examine the influence of the parameters of this problem on the EPC attitude: liquids residuals, initial kinematics conditions, characteristics of the spin-up torques.

A new version of FLOW-3D which deals with the coupled fluid motion and rigid body dynamics was developped (ref.2), enabling us to check the results of the parametrisation.

This paper presents the technological problem, the simplified model, the new version of FLOW-3D, and the results obtained from both codes applied to ArianeV.

Nomenclature

G_f :center of mass of fluid
G_0 :reference point
β : angle between the purge force and the x-axis
ω :angular velocity
Θ :roll angle
q:
α: see figure 3
z:
M : fluid mass
Cf : friction coefficient
Γ: acceleration
$\vec{F}$: force
$\vec{M}$: torque

Subscript:

g :relative to the acceleration
f: relative to the friction
a: absolute
e: training
c: Coriolis
r: relative
DRB: Dry Rigid Body
EPC: Etage Principal Cryotechnique
EPS: Etage à Propergol Stockable

I/ Introduction

After the staging with the Upper stage (EPS), the main cryotechnic stage of ArianeV is spun to get, at the end of the out-atmospheric phase, a transversal angular velocity higher than about 10°/s.

Moreover, in order to avoid all hazards of common bulkhead rupture, it is considered necessary to depressurize the LH2 tank (see fig.1).

To achieve the Stage motion, it seems very convenient to use the purge force. This force depends on the efficiency of the depressurization (throat area, vapor regeneration,...). The other parameters, which can influence the EPC kinematics, are as follows:

- ❒ liquids residuals: M_{LOX} (1), M_{LH2} (2)
- ❒ orientation and location of the depressurization nozzle: F(t) (3), β (4)
- ❒ initial kinematic conditions: ω_x (5), ω_y (6), ω_z (7)
- ❒ Upper Stage plume effects: $\vec{\zeta}$ (8)

This last data is the most difficult to evaluate because it depends on the relative movement of the two stages (EPC and EPS). In the first part of this study, it hasn't be taken into account.

To determine the EPC attitude, an analysis of the propellant movement must be undertaken and the reaction of the fluids and the dry vehicle be computed. The version of FLOW-3D first employed in this study didn't enable one to compute simultaneously the fluids and DRB dynamics. Therefore we chose the following process:

1/ to assess the stage kinematics on time interval τ

2/ to compute the forces and torques exerted by the fluids when submitted to this kinematics

3/ to calculate a new stage kinematics

in taking these fluid torques into account

4/ to compare it to the old and judge the convergence of this interval

5/ to proceed to 1/ once the interval is converged

This method is very complex and moreover, owing to the complexity of FLOW-3D, a trade-off between the accuracy of results and the CPU times was required: τ was chosen large enough to limit the computation time resulting in some loss of accuracy.

To perform the parametric study and propose a depressurization system layout, a simplified model was necessary. This modelization and the main results obtained with it will be described in the following chapter. Then a new version of FLOW-3D was developped by Flow Science, which can compute the coupled dynamics. This extended version permitted us to validate the preceding studies performed with the simplified model, giving us a precise simulation of the entire spin-up phase.

III Simplified Modelization

The main goal of this model is to enable one to determine easily the influence of the parameters which can affect the EPC dynamics. Preliminary computations with FLOW-3D (in which the DRB kinematics is pre-specified) show that:

a/ the LH2 pool oscillates slightly in the bottom of the tank during the whole spin-up, provided that it is located in this area at the beginning of this phase. Indeed, since the depressurization hole is located above the DRB center of mass, the force induces counter action movement on the LH2 liquid and the stage structure as explained in fig.2

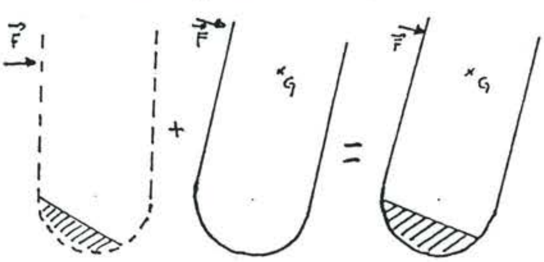

effect on the LH2 pool — effect on the DRB

figure2: relative movement of LH2 and DRB

b/For M_{LOX}=3000kg the pool is not fragmented during the spin-up duration and slides on the tank walls (the impact of the liquid bulk on the baffle doesn't induce fragmentation for this mass which is not true for M_{LOX}=600kg). It can be shown that the greater the LOX residual mass, the more difficult to fulfill the spin-up requirement. Therefore the hypothesis 'fluid not fragmented' is assessed to be conservative for our problem.

It is worth noting that, in these preliminary works, no longitudinal force is taken into account.

1/ Mathematic formulation

Considering these two major results just discussed, the main hypothesis of the simplified code is as follows:

The liquids are modelized as rigid spherical caps able to slide on the structure.

In the following this code will be referred to as "3RB" code (three rigid bodies).

Each tank is subdivided in three areas: lower cap, cylindrical part and upper cap. The movements of the LH2 and LOX centers of mass are so described by the evolution of the parameters q, α, z defined on the figure 3:

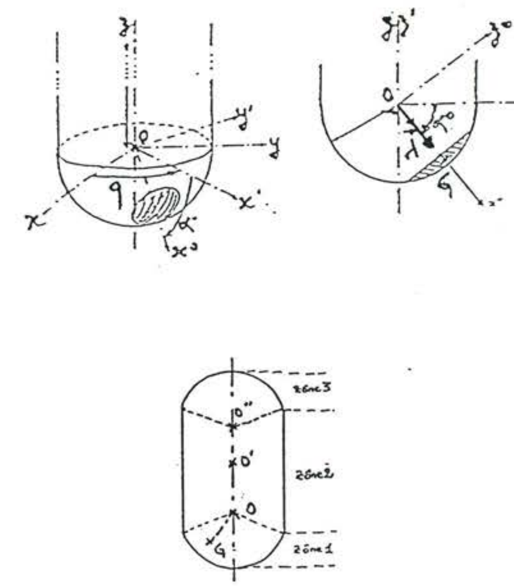

figure3: parameters definition

1/ when the liquid is located in the zone n°1, its movement is assumed to be that of a pendulum oscillating about the fixed point O.

2/ when it moves along the cylindrical walls, it turns around the point O' whose the movement is along the z-axis.

3/ when it reaches the zone n°3, its behaviour is again similar to pendulum's.

Although this model is not very realistic in zone 3 for the LH2, no effort was undertaken to improve it since the LH2 is not likely to reach the common bulkhead (see fig.2).

The GLOX and GLH2 are evaluated by application of the "virtual works" theorem:

$$\delta\zeta_\gamma = \delta\zeta_f \qquad (1)$$

where $$\delta\zeta_\gamma = \int_{fluid} \vec{\Gamma}.\delta\overrightarrow{GM}dm \qquad (2)$$

and

where $$\delta\zeta_f = \int_{fluid} \vec{V^r}.\delta\overrightarrow{GM}dm \qquad (3)$$

$$\vec{\Gamma^a}(M) = \vec{\Gamma^e}(M) + \vec{\Gamma^c}(M) + \vec{\Gamma^r}(M) \qquad (4)$$

$$\vec{V^r}(M) = (\vec{k} \wedge \overrightarrow{OM})\dot{q} + (\vec{\lambda} \wedge \overrightarrow{OM})\dot{\alpha} + \dot{z}\vec{k} \qquad (5)$$

$$\overrightarrow{\delta GM} = (\vec{k} \wedge \overrightarrow{OM})\delta q + (\vec{\lambda} \wedge \overrightarrow{OM})\delta\alpha + \delta z\vec{k} \qquad (6)$$

Developping the equation(1) by taking into account the equations 2 to 6, we get the following relation (7) :

$$\vec{k}dq\int_{fluid}(\overrightarrow{OM} \wedge \overrightarrow{G^a_M}) + \vec{\lambda}d\alpha\int_{fluid}(\overrightarrow{OM} \wedge \overrightarrow{G^a_M}) + dz\int_{fluid}\vec{k}.\overrightarrow{G^a_M} = C_f((\vec{k} \wedge \overrightarrow{OM})^2\dot{q}dq + (\vec{\lambda} \wedge \overrightarrow{OM})^2\dot{\alpha}d\alpha + \dot{z}dz$$

which must be satisfied whatever the values of δq, $\delta\alpha$, δz may be. Therefore we obtain a differential system (I) by separating the coefficients of δq, $\delta\alpha$, δz. in equation (7) :

$$\ddot{q} = f_1(\dot{q}, \dot{\alpha}, z, q, \alpha, z, \overrightarrow{\Gamma^e_{Gf}}, \overrightarrow{\Gamma^a_{G0}})$$

$$\ddot{\alpha} = f_2(\dot{q}, \dot{\alpha}, z, q, \alpha, z, \overrightarrow{\Gamma^e_{Gf}}, \overrightarrow{\Gamma^a_{G0}})$$

$$\ddot{z} = f_3(\dot{q}, \dot{\alpha}, z, q, \alpha, z, \overrightarrow{\Gamma^e_{Gf}}, \overrightarrow{\Gamma^a_{G0}}) \text{ for zone 2}$$

$$\ddot{z} = 0 \qquad \text{for zone1 and 3}$$

Nota: Cf is empirically determined as proposed in the reference 3: $C_f = \sqrt{\dfrac{\rho\mu\Omega}{2}}$

The DRB dynamics is assessed through the general theorem of Solid Mechanics, i.e:

$$M\frac{\delta^2\overrightarrow{OG_{drb}}}{\delta t^2} = \overrightarrow{F_{control}} + \overrightarrow{F_{envir.}} + \overrightarrow{F_{fluid}} \qquad (8)$$

$$\int_{fluid}\overrightarrow{G_0M} \wedge \overrightarrow{\Gamma^a_M}dm + \int_{DRB}\overrightarrow{G_0M} \wedge \overrightarrow{\Gamma^a_M}dm = \vec{\mathcal{M}}(G_0, \overrightarrow{F_{control}}) + \vec{\mathcal{M}}(G_0, \overrightarrow{F_{envir.}}) \qquad (9)$$

The equations 8 and 9 may be written:

system II:

$$\Gamma^a_{XGd} = g1(\omega_x, \omega_y, \omega_z, F^x_{control}, F^x_{envir.}, F^x_{fluid})$$

$$\Gamma^a_{YGd} = g2(\omega_x, \omega_y, \omega_z, F^y_{control}, F^y_{envir.}, F^y_{fluid})$$

$$\Gamma^a_{ZGd} = g3(\omega_x, \omega_y, \omega_z, F^z_{control}, F^z_{envir.}, F^z_{fluid})$$

and

system III:

$$\dot{\omega}_x = f4(\omega_x, \omega_y, \omega_z, q, \alpha, z, \dot{q}, \dot{\alpha}, \dot{z}, \Gamma^a_X, \Gamma^a_Y, \Gamma^a_Z)$$

$$\dot{\omega}_y = f5(\omega_x, \omega_y, \omega_z, q, \alpha, z, \dot{q}, \dot{\alpha}, \dot{z}, \Gamma^a_X, \Gamma^a_Y, \Gamma^a_Z)$$

$$\dot{\omega}_z = f6(\omega_x, \omega_y, \omega_z, q, \alpha, z, \dot{q}, \dot{\alpha}, \dot{z}, \Gamma^a_X, \Gamma^a_Y, \Gamma^a_Z)$$

The systems (I), (II) and (III) constitute a system of differential linear equations which can be solved by the Runge-Kutta method.

2/ First validation

At this step of the study, the model validation could concern only the center of mass of fluid pools and the torques induced by the movement of these mass centers because only the FLOW-3D (without the coupled rigid body dynamics model) was available. Therefore, a simplified model run was performed, using a DRB motion given by kinematics equations. Figure 4 presents the results of the two codes. The difference between results was judged to be acceptably small.

3/ Parametric survey

In order to design the depressurization and spin-up device, a parametric study had to be undertaken. Among the mentioned factors which can affect the EPC are some that depend on the ArianeV performance or general design. Others are closely connected to the depressurization layout.

The behavior of the system must be known at the nominal values of design. Behavior variations resulting from off nominal values are also required.

Figure 5 presents the evolution of the transversal angular velocity, the roll rate and the roll angle for a given data set (parameters 1 through 7) and two values of the initial roll rate.

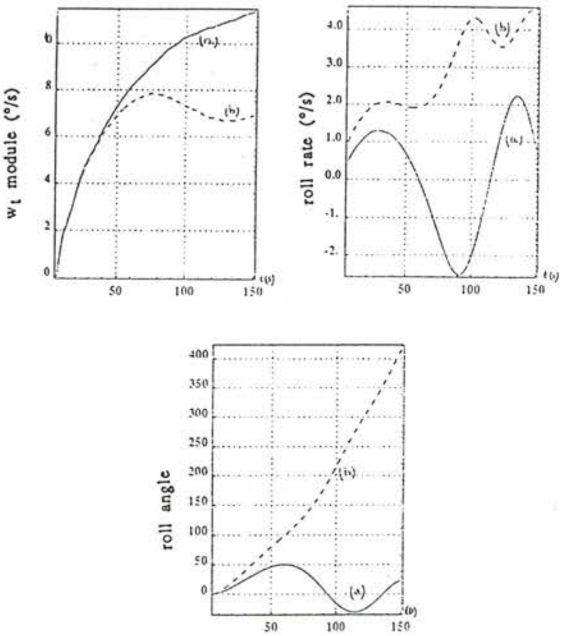

figure5: exemples of spin-up

The results show that there are two types of spin-up:

a/ the roll rate oscillates around zero (case a). In this case the transversal angular speed $\sqrt{\omega_x^2 + \omega_y^2}$ has no maximum value

b/ the roll rate oscillates around a non zero value (case b). In this case w_t is limited by its value at $\Theta = 180°$. This phenomenon is easily explained by the following figure 6:

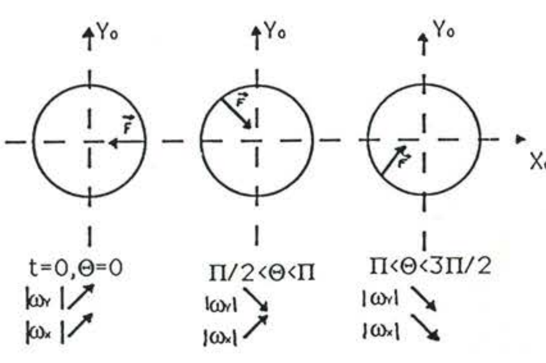

figure6: evolution of ω_t

From figure 6 we conclude that:

+ either the roll angle is restricted to oscillate between -180° and 180°, in which case it is not necessary to formulate a condition about the w_t evolution and there is no restriction on the depressurization device design required to ensure the success of spin-up

+ or the roll angle increases (or decreases) continuously in which case the following condition must be satisfied:

$$\omega_{lim} < \omega_t (\Theta = 360°)$$

where ω_{lim} is the specified value beyond which the success of the mission is warranted.

Of course, in order to be conservative, the spin-up device will be designed to limit the roll velocity. So the parametric study is restricted to the factors which most seriously affect the roll velocity, namely:

. the initial roll velocity

. the location , the diameter and the orientation of the depressurization hole (thrust module).

Our computations have been performed under the following conditions:

* M_{LOX} is the maximum expected residual mass (3000 kg) which corresponds to M_{LH2} =300 kg because:

❒ the stage center of mass is higher and so the torque amplitude is less

❒ the heavier the residual loading, the more difficult it is to achieve the desired spin rate (for a specified depressurization thrust)

* for a given hole diameter, two depressurization thrust module laws can be determined (with and without vapor regeneration). All of the reported computations were performed with the "lower" level.

* the transversal angular velocity is initiated to + 3rad/s (which is the expected limit for ω_t after cut-off of the EPC engine) and opposite to the action of spin-up torque.

These conditions represent the worst case for fulfilling the requirement : $10°/s < \omega_t$

It can be concluded that, under the severe a.m. conditions, the required spin-up will be performed provided that we:

. dispose of the greatest purge force possible during the first minutes. This implies a hole diameter greater than 180 mm.

. limit the creation of roll torque, implying the force orientation will be slightly tilted about x-axis.

. set a sequence so that the depressurization force only spins the EPC. Indeed, in order to depressurize the LH2 tank as soon as possible, it would have been convenient to open the purge hole just after the cut-off the EPC engine (that is, before separation). However, in this case, since the hole is below the center of mass of the Launcher (EPS+EPC as seen in figure1),during the period prior the staging, the resulting torque would have induced a movement of the EPC opposite to that produced after the staging, which might jeopardize the mission success.

Of course, the final design (taken to include the sequence and the passivation device layout) must also take into account the requirement for a positive differential pressure between the LOX and LH2 tanks.

III/ Explicitly Coupled FLOW-3D Model

FLOW-3D is a general purpose, finite-difference solution program that has been widely used (ref. 1) for the analysis of slosh in propellant tanks. It was therefore chosen as the base program whose extension will permit solution of the fully coupled slosh/vehicle dynamics problem.

Several features of the standard version of FLOW-3D are of particular importance with respect to propellant slosh. FLOW-3D treats the movement of propellant tanks through space by imbedding its computational coordinate system in a reference frame fixed within the vehicle. By doing so, FLOW-3D keeps the relative geometry of the tank fixed. However, this strategy leads to a requirement for "fictitious" forces, which represent the motion of the vehicle through inertial space.

The FLOW-3D solution proceeds by a sequence of simple forward difference time steps, using the SOLA algorithm (ref. 2). The first step of SOLA is an explicit approximation of the new time velocity field. The "fictitious" forces are introduced into the solution at this step, together with viscous forces, real gravitational forces, wall shear, and an approximation to the pressure gradient force.

Experience has shown that a completely explicit formulation of the Coriolis terms in the "fictitious" forces can lead to slowly growing numerical instabilities. Therefore, FLOW-3D next implements a 'time-centered' approximation to these terms. This centering averages the coriolis forces based on the fluid velocity from the previous cycle, with those based on the initial estimate of the new velocity field. This stabilizes the solution with regard to the coriolis terms.

The next step of SOLA is to update the fluid pressure field. This update is an iterative process that simultaneously seeks to satisfy the continuity equation. The fluid velocity field is also updated during the iteration process. At all times the solution is required to satisfy the boundary conditions that exist at the edges of the computational mesh, at interfaces with solid materials, and at the liquids/gas interface.

FLOW-3D represents solid material in a somewhat unusual manner. A simple (usually rectangular) mesh is employed. Solids are represented by assigning area fractions to every cell face and volume fractions to each cell. These signify the fraction that is available to fluid. A preprocessor translates simple geometric descriptions of solid bodies into the required area and volume fractions. This method is known as the FAVOR algorithm.

The force and momentum components exerted by the fluid on its containing tank are evaluated by multiplying the fluid pressure times the blocked area of each cell face, summing over all mesh cells. Thus viscous shear forces are not included in this evaluation. Components of torque are evaluated in a similar fashion, accounting, of course, for the necessary lever arm.

At the completion of the iterative evaluation of the pressure field, both pressures and velocities have been fully updated to the next time level. Problems that model confined flow without concern for energy transport, turbulence, or other scalar quantities are therefore completed.

However, the introduction of a free surface into the situation requires an additional step in which the configuration of the surface is updated. In FLOW-3D we use the VOF algorithm (ref. 4) to represent the liquid/gas interface. In VOF a fraction is assigned to each computational cell that represents the fraction of the volume of that cell occupied by liquid. In the free surface model, which is the most frequently used for the slosh analysis, the dynamic solution is only required in the liquid region. The gas space is treated as a region of uniform pressure.

The coupled model implemented for this study is based on the three steps algorithm described above. An additional step is added, which calculates the movement of the vehicle in response to all applied forces and torques. This step occurs after the solution for the new fluid surface. The fluid forces and torques are based on the current values of pressure. These pressures are in turn based in part on acceleration and rotation values derived from the previous motion of the vehicle. This is termed explicit coupling, because each part of the solution is explicitly solved without regard for its effects on the other. This explicit coupling is simple to implement and generally accurate. However it does lead to certain instability limitations, as discussed below.

Naturally, the vehicle is subject to forces and torques that arise from phenomena outside the propellant tanks. In FLOW-3D we have included provisions for two classes of such forces: environmental and control. The division is arbitrary, but is intended to simplify combinations of various effects. A special option is provided for including the attraction due to gravitating body, generally the Earth. Since the direction and distance from this body to the propellant tank will vary during the calculation, FLOW-3D will automatically evaluate its influence as the calculation progresses.

The equations solved for the motion of the vehicle are the classic center of mass and attitude equations. We have chosen to represent the vehicle attitude by the full unitary transformation matrix (A), which allows us to readily transform force, moment, acceleration and rotation vectors between a (presumed inertial) reference frame fixed in the gravitating body and the instantaneous reference frame of the vehicle. The transformation matrix elements are redundant, however, since there are nine of them and only six degrees of freedom, so care must be taken to ensure that they always represent a rotational motion.

Stability

A simple analysis of the dynamics of two solids masses convinces us that the explicit coupling used in FLOW-3D will be unstable under some circumstances. If displacement of body A induces a force on body B while displacement of mass B rigidly accelerates mass A, one can easily show that the mass of A must be less than that of B for stability of an explicit solution of their dynamics. In our case, body A corresponds (approximatively) to the fluid, and B to the vehicle. We strongly suspect that a similar argument can be made regarding the inertial moments of the two components.

Test calculations

A variety of simple test calculations have been performed with the coupled model. These are based on simple harmonic motions (linear and rotational) of solid vehicles with filled spherical tanks. Excellent agreement with approximate analytic solutions was obtained. In one case the stability limitation was verified, although for a fluid mass that slightly exceeded that of the rigid body.

IV/ Comparisons of the two codes- Discussion

Figure 7 presents the results for two depressurization devices configurations obtained with the FLOW-3D extension and the "3RD" model. Each configuration corresponds to a type of roll evolution:

The configuration a/ (depressurization hole is tilted about y-axis) doesn't fulfill the recommandations presented at the end of the chapter II. In this case, the comparaison was performed only to enable us to judge the roll asssesments by the two methods.

The configuration b/ was drawn with respect of the design laws of chapter II. Moreover, in this case, we take into account the Upper Stage plume effects: in fact; with the proposed sequence (the EPC passivation occurs only few seconds after the staging) and the orders of magnitude of the depressurization forces (10kN and a lever arm of 10m) and the plume forces (a mean value of 1.5kN and a low lever arm) the separation rockets affect not greatly the EPC attitude: the fluids configurations described in the figure 8 shows that the main hypothesis of the simplified model are yet valid.

Each calculation was stopped at the point when the success or the failure of the spin-up can be defined:

in configuration a/, the inflection point I1 determines a continuously decreasing of the roll angle

In configuration b/ the roll sign change at t=29s means the roll angle amplitude is restricted to -180°, +180°.

Although the instantaneous roll values evaluated by the two codes are rather different (the difference can raise up to 20%) the roll variations are the same. Moreover it is worth quoting that the "3RB" method seems to be more conservative for our specification than the "FLOW-3D" method. Therefore, these results confirm all the preceding conclusions drawn from the parametric survey and enable to validate the chosen passivation/ spin-up device layout.

VI Conclusion

Although the simplified model allowed for a very large parametric survey with an order of magnitude of the CPU reduction of the order of 10^2, its application is very restrictive and it yields not very precise results.

The FLOW-3D extension accounts for the preceding study and could be used for the flight data reduction. It can also deal with more complex configurations without limitations concerning the exerted forces and torques.

VII References

1- J.M Sicilian, C.W Hirt and R.P Harper, "FLOW-3D: Computational Modeling Power for Scientists and Engineers", FSI-91-001, Flow science Report, 1989.

2- C.W Hirt, "Simplified Solution Algorithms for Fluids Flow Problems", Proceedings of Numerical Methods for Partial Differential Equations Seminar, University of Wisconsin, Academic Press, Inc. 1978.

3- Lamb, "Hydrodynamics", p622,6th Edition, Dover Publications, New York

4-C.W Hirt and B.D Nichols, " Volume of Fluid (VOF) Method for the Dynamics of Free Boundaries", Journal of Computational Physics,39, pg. 201, 1981.

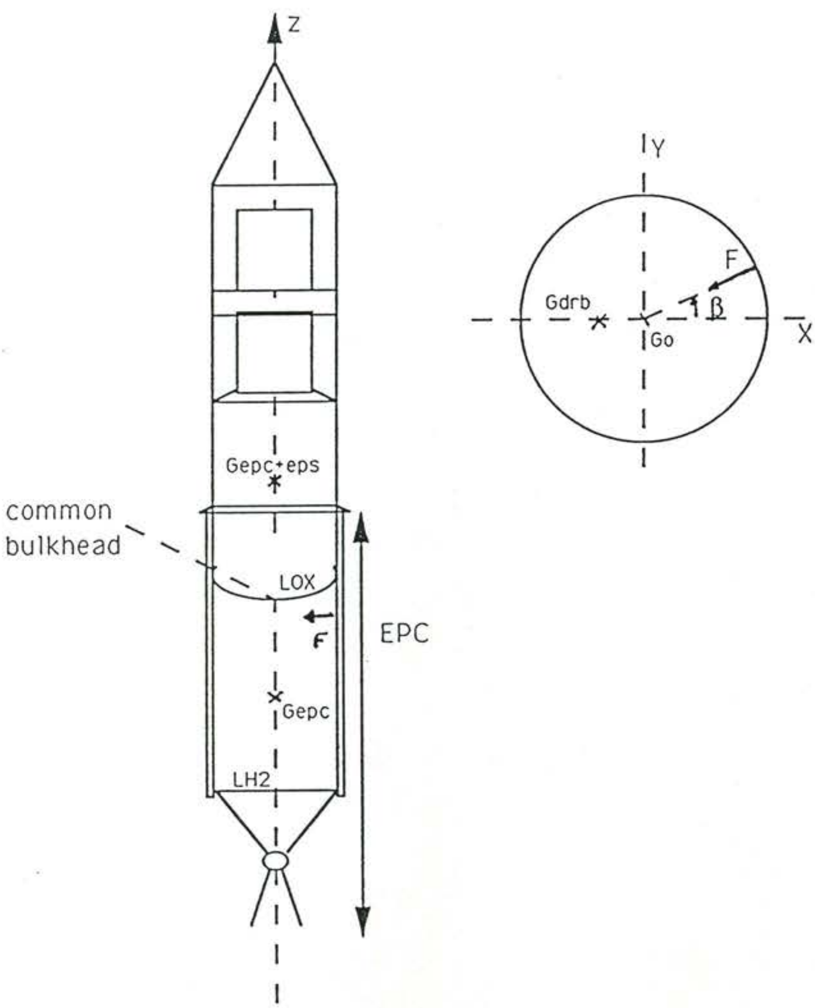

Figure 1: ArianeV configuration. Geometrical data definition

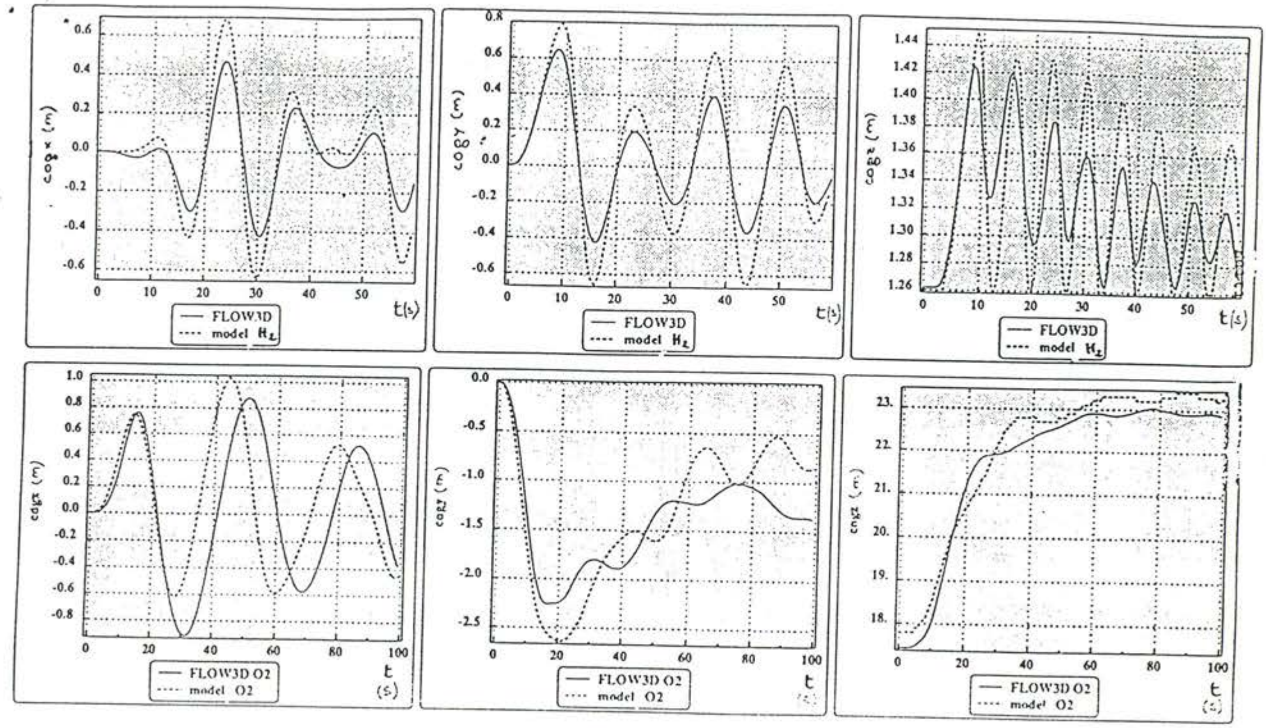

comparison of centers of mass

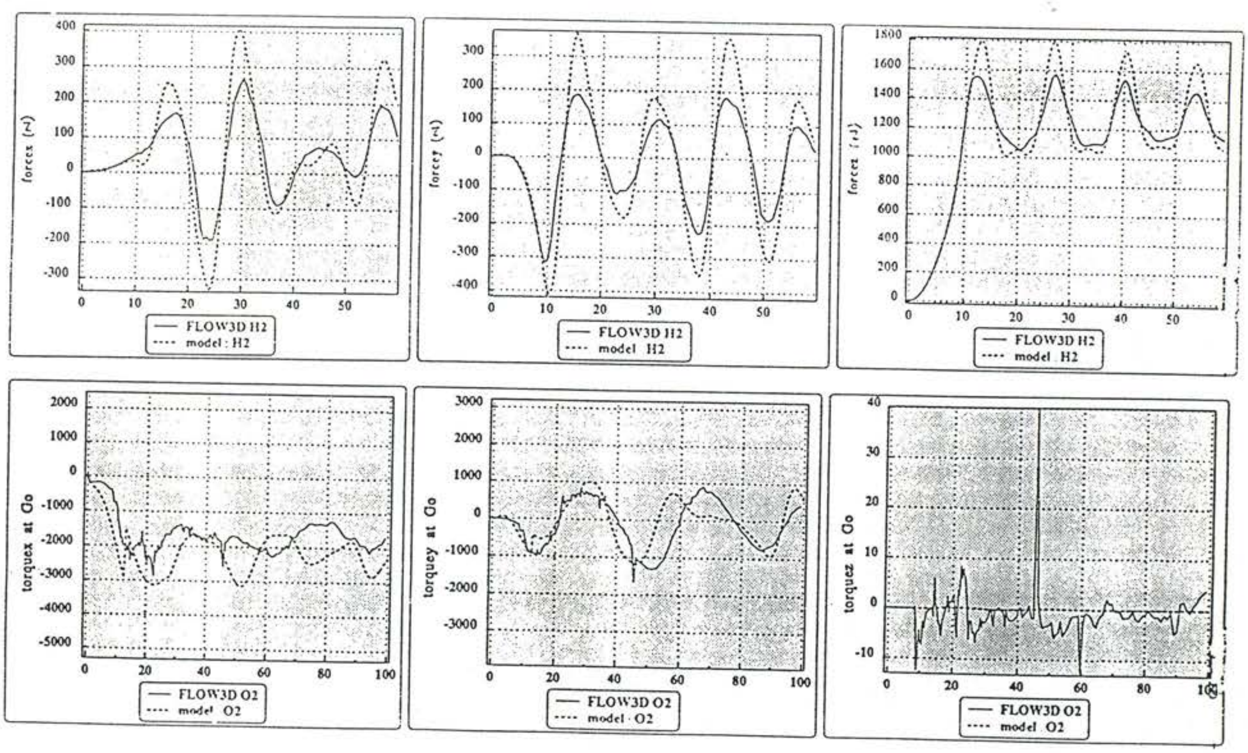

comparison of torques and forces

Figure 4: First comparaison of 3RD and FLOW-3D models

comparison between FLOW-3D and 3RB model : configuration a/

angular velocity (body frame)

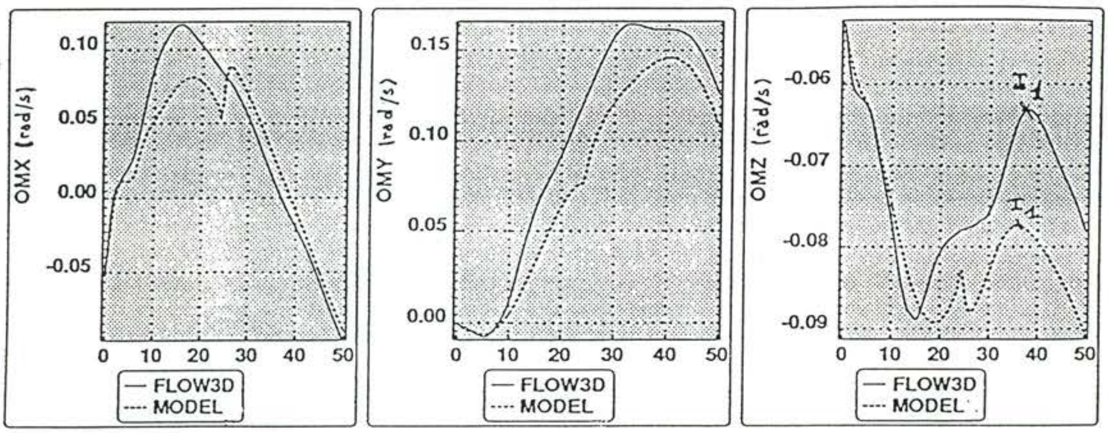

comparison between FLOW-3D and 3RB model : configuration b/

angular velocity

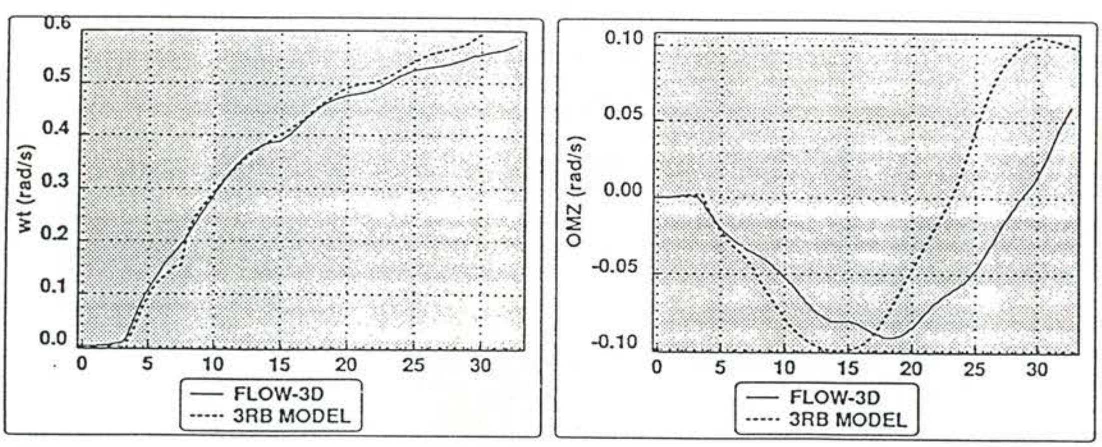

figure 7: comparison FLOW-3D and 3RB for the configurations a and b

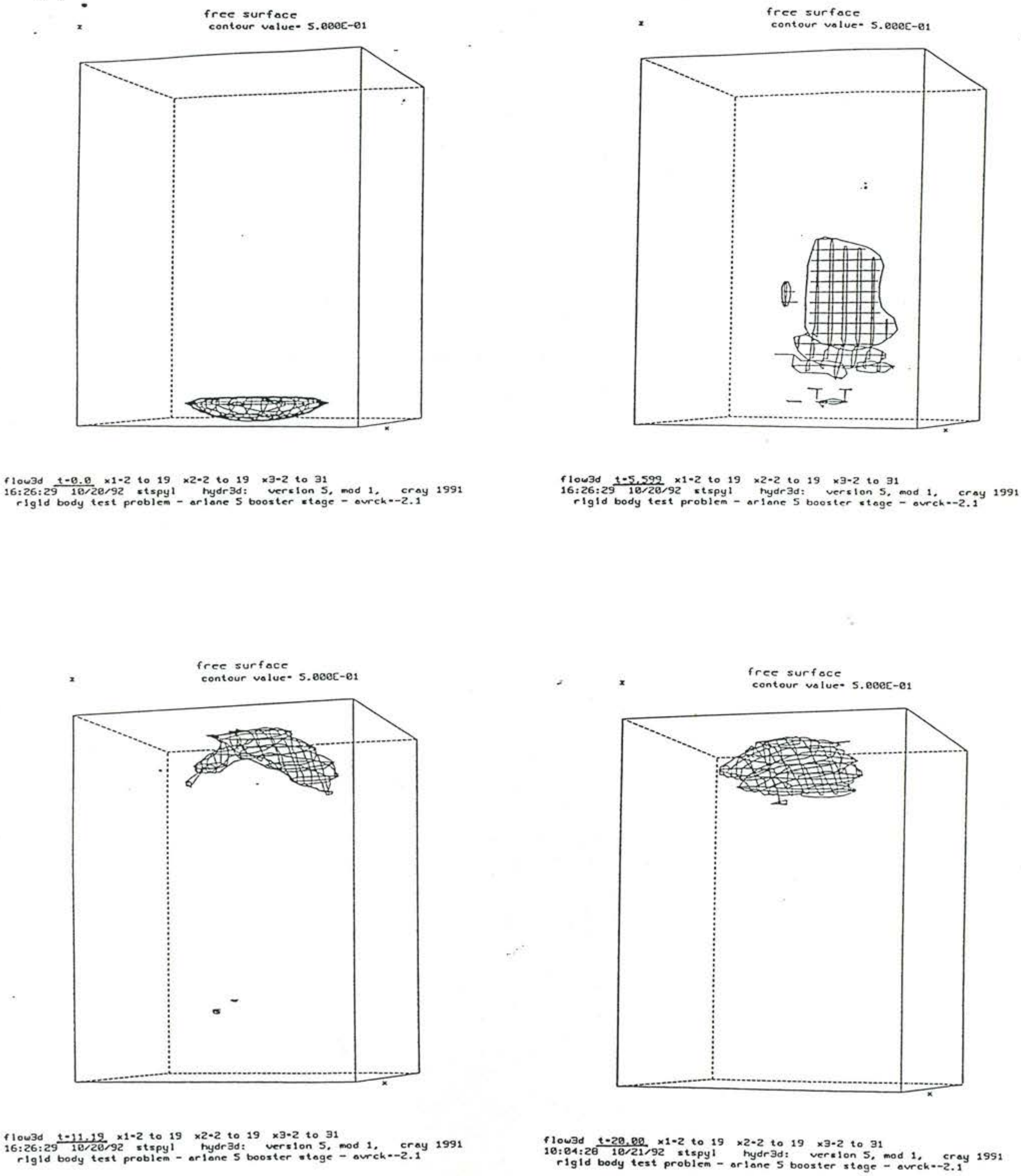

Figure 8 : Flow Patterns for the configuration b/